



## STRUCTURAL AND ELECTRICAL PROPERTIES OF ZnO EMBEDDED IN PANI SOLVENT

Khalaf AL Abdullah<sup>1</sup>, Tarik Zarwri<sup>2</sup>, Wafaa Hajismail<sup>2</sup>

<sup>1</sup>Dept. of Electrical & Electronics Engineering, Aleppo University, Aleppo-SYRIA

<sup>2</sup>Dep of physics, Aleppo University, Aleppo-SYRIA  
[faceeealepuniv@gmail.com](mailto:faceeealepuniv@gmail.com)

Received 14-03-2015, online 11-05-2015

### ABSTRACT

Zinc oxide/polyaniline (ZnO/PANI) hybrid structures have been investigated for their structural and electrical properties. ZnO nanoparticles had prepared by sol-gel method, then pressed in the form of pellets were used for this purpose. The hybrid ZnO/PANI structure was obtained by the addition of PANI on the surface of ZnO. The XRD-pattern of the ZnO modified pellets show shift of peak toward smaller angles so the crystallite size decrease, AC and DC measurements were carried out. The results reveal that the hybrid structures have lower potential barrier height and higher donor density.

**Keyword:** ZnO, electrical properties, XRD

### I. INTRODUCTION

In recent years the manufacture of devices using inorganic/organic hybrid materials has attracted much interest from both the scientific and the technological point of view, improvements in the electronic and the optical properties of these devices are closely related to surface effects. The grain boundaries (a double Schottky barrier could be formed at the grain boundaries) of polycrystalline materials play a significant role in their electrical properties and interfaces, which usually play important roles in device characteristics [1]. Zinc oxide, which is *n*-type semiconductor, with 3.36 eV energy band gap [2], ZnO nanostructures such as nanofibres and nanorods, and nanowire have attracted the attention of several researchers for their potential applications as solar cells, gas sensors, and biosensors. Polyaniline (PANI) is a promising conducting polymer due to ease polymerization environmental stability [3]. PANI is usually considered as a *p*-type semiconductor [4], presence of reactive  $-NH-$  groups in the polymer chain which in parts chemical flexibility to the system and improves the processibility to a large extent [5]. Electrical and optical properties can be changed by oxidation and/or by protonation [1].

Several reports are dealing with the preparation of hybrid materials such as TiO<sub>2</sub>/polyaniline [6], Fe<sub>2</sub>O<sub>3</sub>/polyaniline [7], SnO<sub>2</sub>/polyaniline [8] and ZnO/Polyaniline [9]. PANI is widely used in the area of electrochemical materials, light-emitting diodes, biosensors, chemical sensors, and battery electrodes. In this work ZnO nanoparticales and

ZnO-PANI structures were synthesized. Electrical and structural properties were studied. AC and DC measurements were carried out.

### II. EXPERIMENTAL

#### II. 1 Zinc oxide nanoparticles synthesis:

ZnO nanoparticles were synthesized using sol-gel Technique [10]. Zinc acetate hydrate [(CH<sub>3</sub>COO)<sub>2</sub>Zn·2H<sub>2</sub>O] as precursor and methanol as a solvent were used in the preparation. 0.6 M solution was mixed thoroughly using a magnetic stirrer at temperature at 60°C for 2 h. The clear transparent solution thus obtained was heated at 80°C (higher than the boiling point of methanol) to evaporate the remnant methanol till a white powder (precursor complex) it can be further heat-treated to obtain zinc oxide powder. ZnO was heated at 600°C for 1 h to get ZnO nanoparticles (600 mg) of ZnO powder was compressed in the form of pellets with 1.2 cm in diameter and 1.6 mm in thickness by applying a pressure of (300 Kg/Cm<sup>2</sup>) this sample labeled by Z<sub>0</sub>.

#### II. 2 PANI Synthesis

Polyaniline was synthesized by oxidative polymerization of aniline in the presence of hydrochloric acid using ammonium persulfate (1mol/aqueous hydrochloric acid solution ammonium persulfate as oxidant with an oxidant/aniline molar ratio  $\leq 1.15$  in order to obtain high electrical conductivity yield). The monomer concentration was 1 mol.l<sup>-1</sup>. The solution

temperature was between 0 and 2°C. The reaction was done in 2h. The experimental part consists of adding slowly (even drop by drop) the aqueous ammonium persulfate solution to the aniline/HCl solution, both solutions being pre-cooled to 0°C. The mixture is stirred for about 1 h. Then the formed precipitate filtered and washed many times then it dried [10]. The final obtained material is a polyemeraldine salt.

**II. 3 Preparation of ZnO/PANI interfaces**

In order to form an interface ZnO/PANI, PANI was dissolved in N,N-Dimethylformamide (DMF) which was stirred to obtain a uniform solution. 600mg of ZnO powder was taken and pressed in the form of pellet by applying the previous pressure, then the pellets was obtained at 600°C for 2h. Then pellet was dipping in PANI solution for 24h. and dried at atmospheric condition (sample labeled by Z<sub>1</sub>).

**III. RESULTS AND DISCUSSION**

**III. 1. Structural properties**

X-ray diffraction (XRD) analysis was carried out using XRD LEYBOLD-TYPE 1.03 diffractometer with CuKα radiation of wavelength, λ = 1.5148 Å. Figure (1) shows XRD patterns of samples Z<sub>0</sub>, Z<sub>1</sub>. The presence of prominent peaks shows that the film is polycrystalline in nature. The lattice constant a = 3.0031 Å for Z<sub>0</sub> and a = 2.9941 Å for Z<sub>1</sub>. Crystallite size of the ZnO was calculated by using Scherrer's Formula [11]

$$D = \frac{0.94\lambda}{\beta \cos \theta} \tag{1}$$

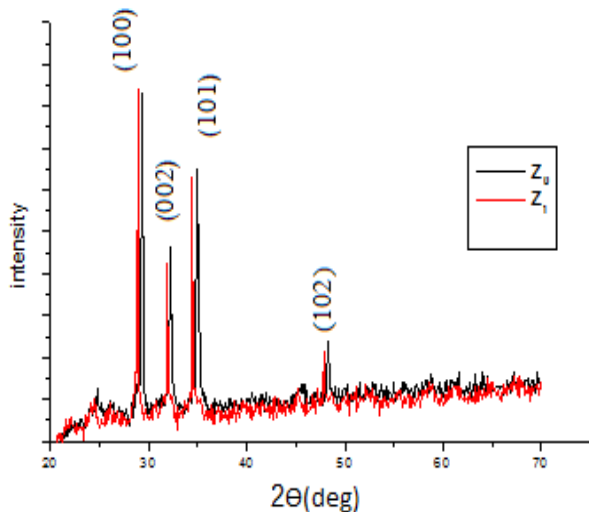


Fig. 1: XRD patterns of Z<sub>0</sub> and Z<sub>1</sub>

where *D* is the crystallite, *λ* is wavelength of the X-ray used, *β* is full width at half maximum intensity (fwhm) in radians and *θ* is the angle of diffraction.

Table (1) crystallite size along prominent diffraction planes.

**Table 1:** crystallite size

	Crystallite Size (nm) along diffraction plane		
	(100)	(002)	(101)
Z <sub>0</sub>	16.831	16.829	9.706
Z <sub>1</sub>	10.527	9.4302	10.678

**III. 2 DC-measurements**

**III. 2.1 I-V Characteristics**

I-V characteristics were recorded using high resistance meter type MEGOHMETER (M1500P). Figure (2) shows I-V characteristics for Z<sub>0</sub>, Z<sub>1</sub> samples which reveal that sample Z<sub>1</sub> has higher current than the current of Z<sub>0</sub> (pure ZnO).

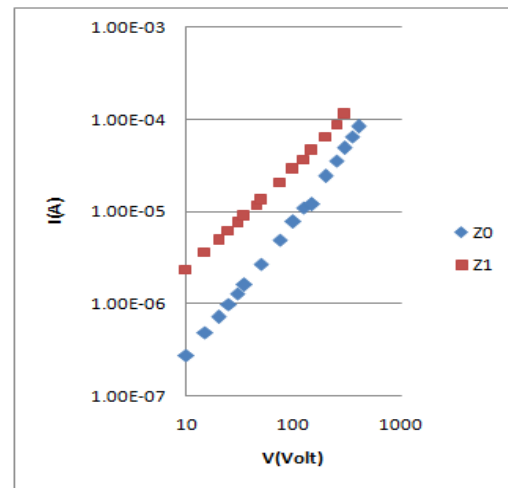
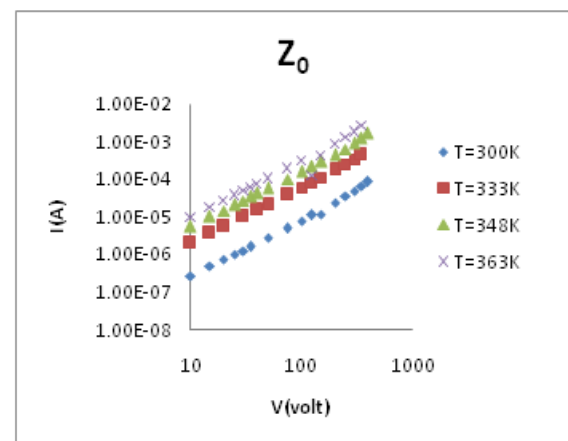


Fig. 2: I-V characteristics of samples

**III. 2.2 Barrier height determination:**

Figure (3) and figure (4) show I-V curves measured at different temperatures (333, 348, 363)K.



**Fig. 3:** I-V curves of  $Z_0$  with different temperatures

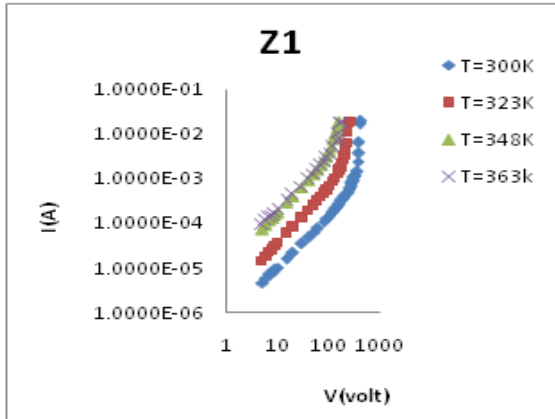


**Fig. 4:** I-V characteristics of  $Z_1$  for different temperatures

Potential barrier height  $\Psi$  can be calculated by using Arhenius relationship [12]

$$I = I_0 e^{-\Psi/KT} \quad (2)$$

K is Boltzman Constant and T is temperature.

By plotting  $\ln(I)$  in function of  $1/T$ ,  $\Psi$  can be determinate from the slope of the resulting line. Figure (5) and figure (6) show potential barrier height as function of potential.

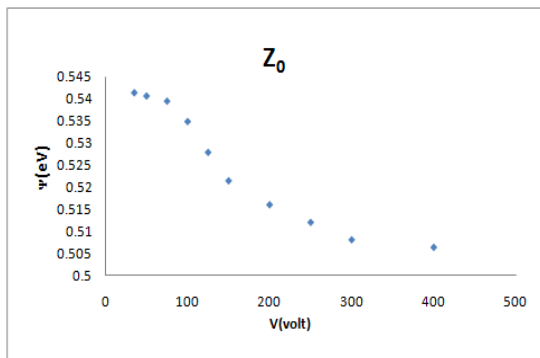


**Fig. 5:** barrier values for different potentials for  $Z_0$

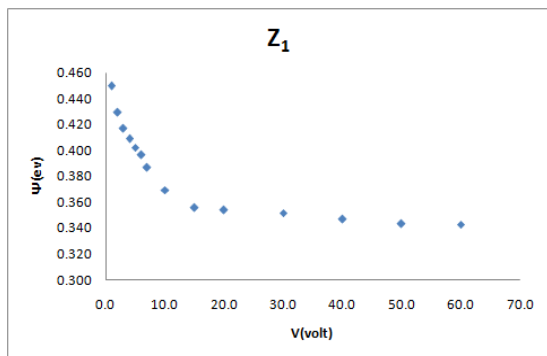


**Fig. 6:** barrier values for different potentials for  $Z_1$

The barrier height decreases in  $Z_1$  and the value of barrier height is lower than that of  $Z_0$ . This might be due to polyaniline affects the ZnO. Interfacial interactions occurring between ZnO and PANI resulted in decrease of the potential barrier height between ZnO grains .

### III. 3 Ac-measurements:

Ac-measurements were carried out with a LCR meter and figure (7) shows the resistances of  $Z_0$ ,  $Z_1$  as functions of  $\log(\omega)$ .

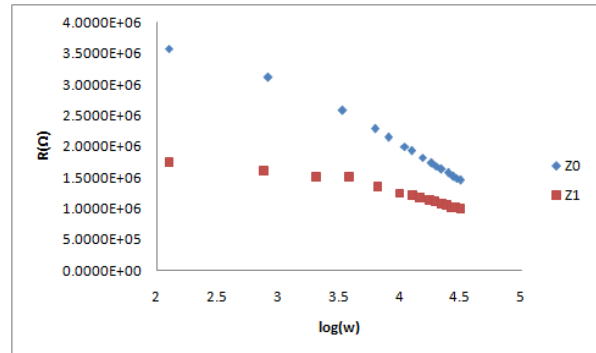


**Fig. 7:**  $Z_0$ ,  $Z_1$  resistances as function of  $\log(\omega)$

Capacitance  $C_p$  as function of AC frequency signal  $\log(\omega)$  was carried out and seen in figure (8) and figure (9) [13] The trapped electric charge follows the applied voltage oscillations and contributes to the total capacitance only if their frequency does not exceed the characteristic trap frequency  $\omega_t$ . Therefore, in the case of low frequencies  $\omega \ll \omega_t$ , the trap related capacitance  $C_t$  is equal to the low frequency capacitance where the deep and shallow trap contributes to capacitance. In high frequency ( $\omega \gg \omega_t$ ) measurements the junction capacitance  $C_s$  is the high frequency capacitance where the shallow trap contributes to capacitance. Table (2) shows the  $C_t$  and  $C_s$  values of  $Z_1$  and  $Z_0$ .

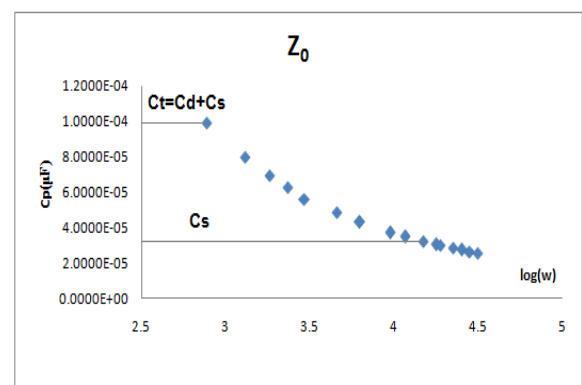


**Fig. 8:** capacitance  $C_p$  as a function of  $\log(\omega)$  for  $Z_0$

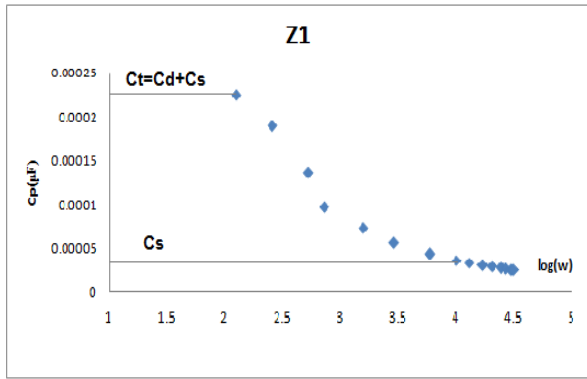


**Fig.9:** capacitance  $C_p$  as a function of  $\log(\omega)$  for  $Z_1$

**Table 2:**  $C_t, C_s$  value of  $Z_1, Z_0$ .

	$C_{tot}=C_s+CD(F)$	$C_s(F)$
$Z_0$	99.072E-12	31.855E-12
$Z_1$	22.4E-11	36.256E-12

**III. 3.1 C-V characteristics:**

Mott-Schottky measurements are the common method for studying the capacitive behavior of a double Schottky barrier. It is possible to obtain information about average donor density, based on the following [14] equation

$$\left(\frac{1}{C_p} - \frac{1}{C_p^0}\right)^2 = \frac{1}{2q\epsilon_s(N_d - N_a)}(V + \phi_b) \quad (3)$$

where  $C_p$  is the capacitance per unit area of a grain boundary,  $C_p^0$  is the capacitance per unit area when  $V=0$ ,  $q$  is the electron charge,  $\epsilon_s$  is the dielectric constant of zinc oxide,  $N_d$  is the donor density,  $\phi_b$  is the barrier height, and  $V$  is the applied voltage per grain boundary. By plotting  $\left(\frac{1}{C_p} - \frac{1}{C_p^0}\right)^2$  versus the applied voltage figure (10) and figure (11) it is possible to calculate  $N_d$  from the slope of the lines and then the traps density  $N_t$ .

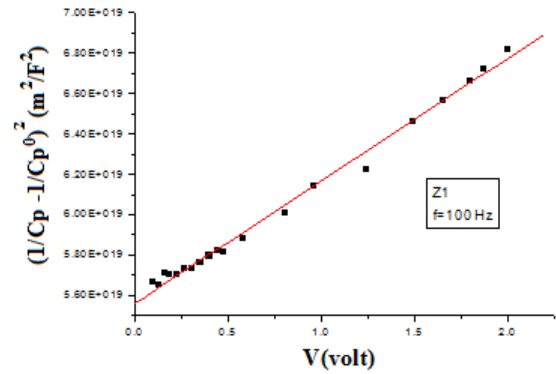


**Fig. 10:**  $(1/C - 1/C_0)^2$  vs  $V$  for sample  $Z_0$  at  $F=100\text{Hz}$ .

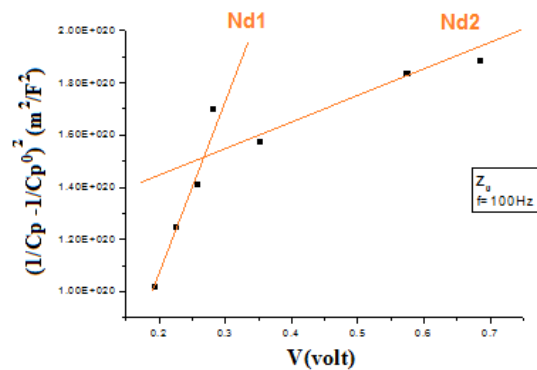


**Fig. 11:**  $(1/C - 1/C_0)^2$  vs  $V$  for sample  $Z_0$  at  $F=100\text{Hz}$ .

From figure (7)  $Z_0$  shows two donor levels so it have two values of donor density  $N_d$  and both are lower than that of  $Z_1$  table (3) include donor intensity and trap density of  $Z_0, Z_1$ .

**Table3:** donor intensity and trap density of  $Z_0$  and  $Z_1$

F=100Hz		
	$N_d(\text{cm}^{-3})$	$N_t(\text{Cm})^{-2}$
$Z_0$	2.226E+08	3.362E+08
$Z_0$	3.622E+09	1.365E+09
$Z_1$	2.727E+10	2.952E+10

#### IV. CONCLUSION

ZnO/PANI hybrid interface was prepared by dipping ZnO pellets in PANI solvent for 24 hours. Observation of this study reveals that the polyaniline affects ZnO. Interfacial interactions occurring between ZnO and PANI resulted in cohesion of PANI molecules with oxide matrix. Organic-inorganic hybrids so formed represent materials which can be used in many applications.

#### Acknowledgement

Thanks to Dr. M.A. Batal for his help in reading the manuscript.

#### References

- [1] Eronides F., da Silva Jr., Elder A. de Vasconcelos., Eronides F. da "Tailoring the Electrical Properties of ZnO/Polyaniline Heterostructures for Device Applications" Journal of the Korean Physical Society **58**, 1256-1260 (2011).
- [2] Nanda Shakti, P.S.Gupta "Structural and Optical Properties of Sol-gel Prepared ZnO Thin Film", Applied Physics Research **2**, 19-28 (2010).
- [3] Shahid Pervez Ansari, Faiz Mohammad "Electrical Studies on the Composite of Polyaniline with Zinc Oxide Nanoparticles", The IUP Journal of Chemistry III **4**, 7-18 (2010).
- [4] Mansi Dhingra., Lalit Kumar, Sadhna Shrivastava, P Senthil Kumar, S Annapoorni, "Impact of interfacial interactions on optical and ammonia sensing in zinc oxide/polyaniline structures", Bull. Mater. Sci. **36**, 647-652 (2013).
- [5] Sadiya Ameen., Chulgi Jo., Young Soon Kim., Hyung-Shik Shin, "Heterostructure Formation of Polyaniline/ZnO Nanoparticulate Thin Film Using Electrophoretic Deposition Technique", Theories and Applications of Chem. **16**, 557-560 (2010).
- [6] Ali Olad, Sepideh Behboud, Ali Akbar Entezam, "Preparation characterization and photocatalytic activity of TiO<sub>2</sub>/polyaniline core-shell nanocomposite", Bull. Mater. Sci, **35**, 801-809 (2012).
- [7] Syed Khasim, S C Raghavendra, M Revanasiddappa, K C Sajjan, Mohana Lakshmi and Muhammad Faisal, "Synthesis, characterization and magnetic properties of polyaniline/Fe<sub>2</sub>O<sub>3</sub> composites", Bull. Mater. Sci. **34**, 1557-1561 (2011).
- [8] S. B. Kondawar, S. P. Agrawal, S. H. Nimkar, H. J. Sharma, P. T. Patil, "Conductive polyaniline-tin oxide nanocomposites for ammonia sensor", Advanced Materials Letters **3**, 393-398 (2012).
- [9] Ömer Sinan Şahin, Ahmet AVCII, Erkan Aydin1, Handan Gulce, Ahmet Gulce, "Production and Characterisation of ZnO-Polyaniline Nano Composites", 6th International ECNP Conference, Madrid (Spain) 28-30 April, 28-30 (2010).
- [10] Dominique Nicolas Debarnot., Fabienne Poncin Epailard", Polyaniline as a new sensitive layer for gas sensors", Analytica Chimica Acta **475**, 1-15 (2003).
- [11] Cullity B.D., Stock, S.R. (2001). "Elements of X-Ray diffraction" (3rd Ed.), Prentice Hall.
- [12] Dorlance O.; Tao M., World congress on high Tech, Ceram, 6<sup>th</sup> Ed (1986), Italy, p. 1809.
- [13] Poonam Rani Kharangarh, ".Study of deep level defects of n+-CdS/p-CdTe solar cells", thesis, Doctor of Philosophy Applied Physics (2013).
- [14] K. Vojisavljević., M. Žunić., G. Branković, T. Srećković, "Electrical Properties of Mechanically Activated Zinc Oxide", Science of Sintering **38**, 131-138 (2006).
- [15] S. Rajesh, T. Ganesh, Francis P. Xavier, "Thickness dependent micro structure, optical and conducting properties of ZnO thin films by spin coating process", Journal of Electron Devices **17**, 1417-1422 (2013).